Developmental Cell
Short Article

The Snail Family Member Worniu Is Continuously Required in Neuroblasts to Prevent Elav-Induced Premature Differentiation

Sen-Lin Lai,[1] Michael R. Miller,[1] Kristin J. Robinson,[1] and Chris Q. Doe[1,*]
[1]Institute of Neuroscience, Institute of Molecular Biology, Howard Hughes Medical Institute, University of Oregon, Eugene, OR 97403, USA
*Correspondence: cdoe@uoneuro.uoregon.edu
http://dx.doi.org/10.1016/j.devcel.2012.09.007

SUMMARY

Snail family transcription factors are best known for regulating epithelial-mesenchymal transition (EMT). The *Drosophila* Snail family member Worniu is specifically transcribed in neural progenitors (neuroblasts) throughout their lifespan, and *worniu* mutants show defects in neuroblast delamination (a form of EMT). However, the role of Worniu in neuroblasts beyond their formation is unknown. We performed RNA-seq on *worniu* mutant larval neuroblasts and observed reduced cell-cycle transcripts and increased neural differentiation transcripts. Consistent with these genomic data, *worniu* mutant neuroblasts showed a striking delay in prophase/metaphase transition by live imaging and increased levels of the conserved neuronal differentiation splicing factor Elav. Reducing Elav levels significantly suppressed the *worniu* mutant phenotype. We conclude that Worniu is continuously required in neuroblasts to maintain self-renewal by promoting cell-cycle progression and inhibiting premature differentiation.

INTRODUCTION

Stem cells must remain proliferative without becoming tumorigenic, and must remain competent to differentiate without actually differentiating. How stem cells maintain stemness—cell survival, cell-cycle progression, and the capacity to differentiate—is a widely relevant question with clinical significance. *Drosophila* neural progenitors (neuroblasts) have become a good model system to study how neural stem cells self-renew and maintain stem cell identity. Larval neuroblasts undergo repeated rounds of asymmetric cell division, each time generating a smaller differentiating daughter cell and a larger self-renewing neuroblast (Doe, 2008). During neuroblast division, many proteins are asymmetrically partitioned into the neuroblast or daughter cell, where they often contribute to neuroblast self-renewal or daughter cell differentiation (Knoblich, 2008), but much less is known about the transcriptional program that maintains neuroblast self-renewal.

Worniu (Wor) is a zinc finger transcription factor in the "Slug/Snail" family, and is transcribed in neuroblasts from the time of their birth. Over 50 Snail family members have been characterized in metazoans; they can directly bind DNA, RNA, or protein and regulate a wide range of cellular functions (Nieto, 2002; Thiery et al., 2009). Snail family members are best known for inducing epithelial-mesenchymal transition (EMT) during mesoderm development and neural-crest cell formation (Barrallo-Gimeno and Nieto, 2005; Cano et al., 2000). In *Drosophila*, four Snail family genes are known: *wor*, *escargot*, *snail*, and *scratch* (Ashraf and Ip, 2001; Roark et al., 1995). The genes *wor*, *escargot*, and *snail* are expressed in neuroectoderm during embryogenesis to trigger EMT in neuroepithelial cells and transform them into newly-delaminated neuroblasts (Ashraf et al., 1999). Wor, Escargot, and Snail also act redundantly to promote expression of the apical polarity gene *inscuteable* (*insc*) and the cell-cycle regulator *string* in newly formed embryonic neuroblasts (Ashraf and Ip, 2001; Cai et al., 2001).

The only Snail family member known to be expressed continuously in neuroblasts is Wor, but its function beyond neuroblast formation has not been investigated. Here we show that Wor maintains neuroblast self-renewal via dual functions: it promotes cell-cycle progression (specifically the prophase-to-metaphase transition) and it inhibits premature differentiation (by suppressing Elav protein levels). These functions occur in neuroblasts well after their formation, highlighting the potential role of Snail family members in stem cell self-renewal.

RESULTS

To analyze the *wor* mutant phenotype we used a deficiency that removes *wor* and several flanking genes, *Df(2L)Exel8034*, and a specific mutation within the *wor* gene, wor^1 (Ashraf et al., 2004). We sequenced wor^1 and found two missense mutations (Figure S1 available online), one of which alters the amino acid Pro443 to Ser in the conserved zinc finger domain and probably changes the conformation for DNA/RNA/protein binding. Because wor^1/wor^1 had a slightly weaker phenotype compared to $wor^1/Df(2L)Exel8034$ due to lesser amount of Wor protein in the latter genotype, we conclude that wor^1 is a strong hypomorph. We use $wor^1/Df(2L)Exel8034$ for all experiments below (called "*wor* mutants").

TU-Tagging/RNA-seq Shows that *worniu* Mutant Neuroblasts Downregulate Neuroblast Genes and Upregulate Neuronal Differentiation Genes

Wor protein is nuclear and is predicted to be a transcription factor, so we compared the transcriptional profile of wild-type

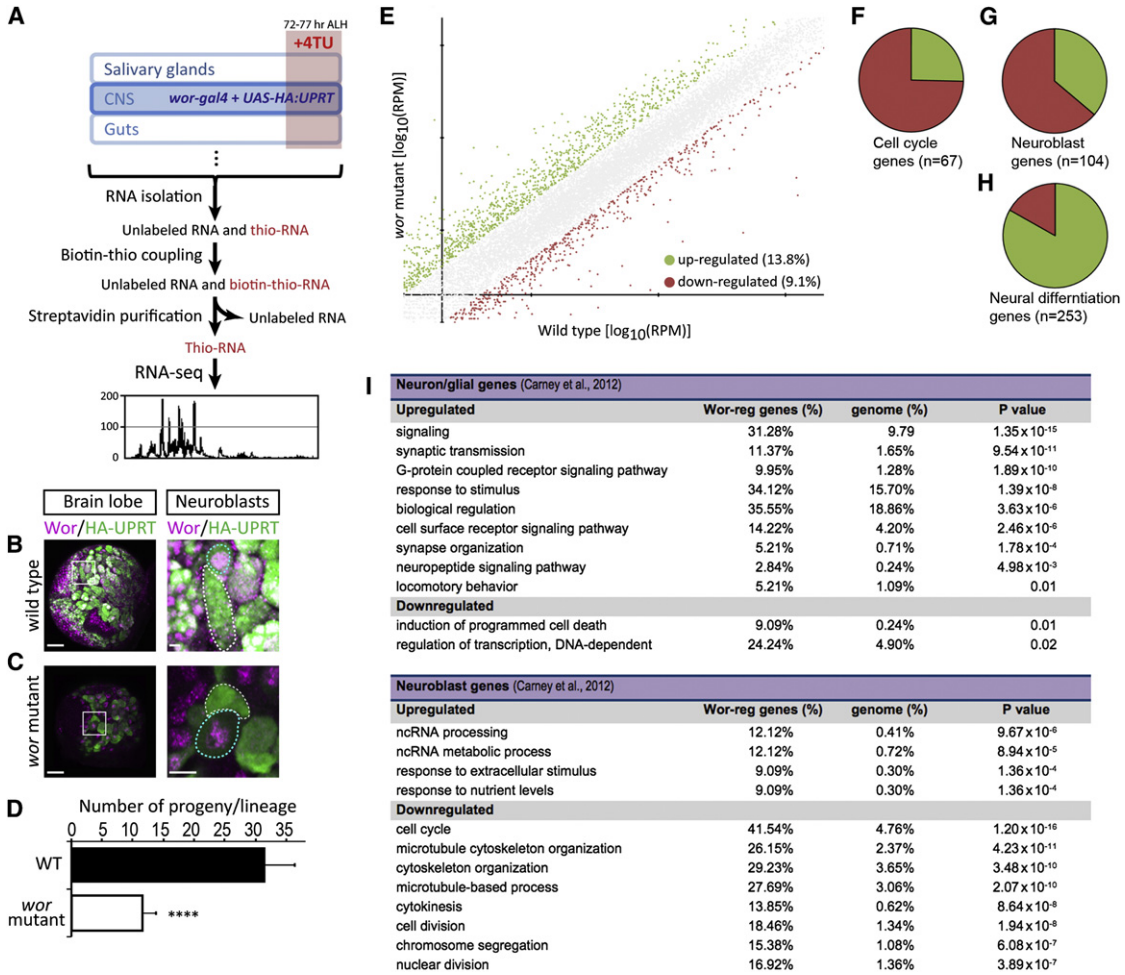

I

Neuron/glial genes (Carney et al., 2012)			
Upregulated	**Wor-reg genes (%)**	**genome (%)**	**P value**
signaling	31.28%	9.79	1.35×10^{-15}
synaptic transmission	11.37%	1.65%	9.54×10^{-11}
G-protein coupled receptor signaling pathway	9.95%	1.28%	1.89×10^{-10}
response to stimulus	34.12%	15.70%	1.39×10^{-8}
biological regulation	35.55%	18.86%	3.63×10^{-6}
cell surface receptor signaling pathway	14.22%	4.20%	2.46×10^{-6}
synapse organization	5.21%	0.71%	1.78×10^{-4}
neuropeptide signaling pathway	2.84%	0.24%	4.98×10^{-3}
locomotory behavior	5.21%	1.09%	0.01
Downregulated			
induction of programmed cell death	9.09%	0.24%	0.01
regulation of transcription, DNA-dependent	24.24%	4.90%	0.02

Neuroblast genes (Carney et al., 2012)			
Upregulated	**Wor-reg genes (%)**	**genome (%)**	**P value**
ncRNA processing	12.12%	0.41%	9.67×10^{-6}
ncRNA metabolic process	12.12%	0.72%	8.94×10^{-5}
response to extracellular stimulus	9.09%	0.30%	1.36×10^{-4}
response to nutrient levels	9.09%	0.30%	1.36×10^{-4}
Downregulated			
cell cycle	41.54%	4.76%	1.20×10^{-16}
microtubule cytoskeleton organization	26.15%	2.37%	4.23×10^{-11}
cytoskeleton organization	29.23%	3.65%	3.48×10^{-10}
microtubule-based process	27.69%	3.06%	2.07×10^{-10}
cytokinesis	13.85%	0.62%	8.64×10^{-8}
cell division	18.46%	1.34%	1.94×10^{-8}
chromosome segregation	15.38%	1.08%	6.08×10^{-7}
nuclear division	16.92%	1.36%	3.89×10^{-7}

Figure 1. TU-Tagging/RNA-seq Shows that *wor* Mutants Downregulate Neuroblast Genes and Upregulate Neuronal Differentiation Genes

(A) Scheme of TU-tagging processes for transcriptome analysis. 4TU, 4-thioruacil.

(B–D) Wild-type and *wor* mutant NBs both express HA-tagged UPRT (HA:UPRT) in third instar larvae. In both (B) and (C), the left panel is a low magnification view of a brain lobe (scale bar represents 20 μm) with the boxed region shown at high magnification (scale bar represents 5 μm) in the right panels. HA:UPRT is expressed in NB (cyan dotted circles in the right panels) and persists in the newborn neuroblast progeny (dotted white circles in right panels); quantified in (D). ****p value < 0.0001. Small Wor+ cells adjacent to neuroblasts are newborn GMCs.

(E) Log to the base 10 of fold of gene activities in WT and *wor* mutants. Green dots are genes upregulated more than 2-fold; red dots are genes downregulated more than 2-fold.

(F) Pie chart represents the 67 of the 586 *Drosophila* "cell cycle" annotated genes (GO:0007049) that are differentially regulated in *wor* mutants (>2-fold or <2-fold change); the majority are downregulated (75%; red) and a minority are upregulated (25%; green).

(G and H) Pie charts represents the "neuroblast" genes or the "neuron differentiation" genes from Carney et al. (2012) that are differentially regulated in *wor* mutants (>2-fold or <2-fold change). The majority of the 253 "neuron differentiation" genes are upregulated (85%; green); whereas the majority of the 104 "neuroblast" genes are downregulated (66%; red).

(I) GO terms that whose frequency is over-represented in *wor* upregulated (>2-fold) or *wor* downregulated (<2-fold) genes compared to their frequency in the genome. Only genes within the "neuron differentiated" (top) or "neuroblast" (bottom) gene lists from Carney et al. (2012) are analyzed.

See also Figure S1 and Tables S1 and S2.

(WT) and *wor* mutant neuroblasts to identify biological processes that were regulated by Wor. We used the TU-tagging method (Miller et al., 2009) to identify mRNAs that are actively transcribed in WT or *wor* mutant neuroblasts. TU-tagging is a spatial/temporal intersectional method to purify nascent RNA from designated tissues during a specific developmental stage (summarized in Figure 1A). We expressed UPRT in larval neuroblasts using *wor-gal4* (Cabernard and Doe, 2009; Lee et al., 2006; Miller et al., 2009), which produced a high level of UPRT in WT and *wor* mutant larval neuroblasts (Figures 1B and 1C, dotted cyan circles) with some persistence into their newborn progeny (Figures 1B and 1C, dotted white circles, quantified in 1D).

We fed early third instar larvae 4TU for 5 hr beginning at 72 hr after larval hatching (ALH) and then purified thio-labeled RNA, performed RNA-sequencing, and designed a custom computational pipeline to analyze the results. We performed two replicates from *wor* mutants and two from WT. We mapped an average of 5.49 million reads from WT and 5.35 million reads

from *wor* mutants. A comparison of the averaged WT versus averaged *wor* data showed that *wor* mutants had 13.8% of genes upregulated at least 2-fold and 9.1% of genes downregulated at least 2-fold (Figure 1E; Table S1).

We first analyzed the upregulated genes. We found that genes upregulated in *wor* mutants were enriched for gene ontology (GO) terms linked to neuronal differentiation such as G protein coupled receptor signaling, sensory perception, serotonin receptor signaling, and synaptic transmission (Table S2). In addition, we recently defined a group of "neuronal differentiation genes" in a transcriptomic analysis of larval brains enriched for neuroblasts or neurons (Carney et al., 2012). We found that 253 of the ~1,100 "neuronal differentiation" genes were differentially regulated in *wor* mutants (>2-fold or <2-fold), with a strong bias toward being upregulated (Figure 1H). GO analysis of the upregulated genes shows significant overrepresentation of the terms signaling, synaptic transmission, synapse organization, and neuropeptide signaling pathway categories (all $p < 0.005$; Figure 1I). We conclude that *wor* mutant neuroblasts aberrantly upregulate neuronal differentiation genes.

We next analyzed the downregulated genes. We asked whether previously defined "neuroblast genes" or "cell cycle genes" are downregulated in *wor* mutant neuroblasts—the converse of the observed upregulation of neuronal differentiation genes. We found that 104 of the ~970 "neuroblast" genes from Carney et al. (2012) were differentially expressed in *wor* mutants (>2-fold or <2-fold), with a strong bias toward being downregulated (Figure 1G). The downregulated genes had a highly significant over-representation of the GO terms cell cycle, microtubule cytoskeleton organization, cytokinesis, cell division, and chromosome segregation (all $p < 0.000001$; Figure 1I). Similarly, we found a downregulation of *Drosophila* genes annotated as "cell cycle": of the 586 cell cycle annotated genes (GO:0007049), 67 were differentially regulated in *wor* mutants versus WT, and most (74.6%) were downregulated (Figure 1F). We conclude that *wor* mutant neuroblasts fail to properly express "neuroblast" genes including those regulating the cell cycle.

Worniu Maintains Neuroblast Stemness by Promoting Cell Cycle, Cortical Polarity, and Survival

Based on our transcriptomic analysis, we predicted that *wor* mutant neuroblasts would show defects in neuroblast attributes (cell-cycle progression, cell polarity, and survival) and precocious neural differentiation. All of these phenotypes could lead to the smaller brain size and reduced neuroblast numbers observed in *wor* mutants (Ashraf et al., 2004; Figures 2A and 2B).

Worniu Promotes Neuroblast Cell-Cycle Progression

To determine whether *wor* mutant neuroblasts have a normal cell cycle, we performed EdU incorporation and counted the number of EdU+ neuroblasts immediately after the pulse. In this and subsequent experiments, we identify larval neuroblasts as large (>8 μm) Dpn+ cells within the central brain; optic lobe neuroblasts were not characterized. Most WT neuroblasts were EdU+ (Figure 2C, green bar), consistent with their reported cell cycle time of ~2 hr (Cabernard and Doe, 2009). In contrast, very few *wor* mutant neuroblasts were EdU+ (Figure 2C, red bar), indicating a cell-cycle delay between G2-M-G1. To determine if the *wor* mutants were delayed in mitosis, we measured the mitotic index of WT and *wor* mutant brains by staining for the M-phase marker phosphohistone H3 (PH3). By late third instar (96–120 hr ALH) there was a striking increase in the PH3+ neuroblasts in *wor* mutant compared to WT (Figure 2D). We conclude that third instar *wor* mutant neuroblasts have a delay in completing mitosis.

To determine more precisely the nature of the M-phase delay in *wor* mutants, we performed live imaging of neuroblast mitosis within the intact brain (Cabernard and Doe, 2009; Cabernard et al., 2010; Siller et al., 2005, 2006). We imaged third instar larval neuroblasts expressing both His2A:RFP to monitor chromosomes (Schuh et al., 2007) and Zeus:GFP to image spindle microtubules (Cabernard and Doe, 2009). Wild-type neuroblasts showed the expected mitosis length of ~20 min (Cabernard and Doe, 2009; Siller and Doe, 2008; Siller et al., 2005) (Figure 2E, quantified in 2H). In contrast, *wor* mutant neuroblasts showed a dramatically extended prophase and/or prometaphase (Figures 2F and 2G; quantified in 2H). We also observed failure in centrosomal separation and bent mitotic spindles. In two cases we observed neuroblasts that "escaped" prophase arrest, and these had a relatively normal length of anaphase (Figure 2H, top two neuroblasts). We conclude that *wor* mutant neuroblasts show an arrest or delay in the prophase/metaphase transition, a stage of the cell cycle where microtubules are dramatically reorganized (see Discussion).

Worniu Promotes Neuroblast Cortical Polarity

We have previously observed cell-cycle delays in neuroblasts lacking aPKC or Dap160 apical cortical polarity proteins (Chabu and Doe, 2008), and *wor-escargot-snail* triple null mutants lack apical localization of Insc in embryonic neuroblasts (Ashraf and Ip, 2001). We stained for apical and basal polarity proteins, and observed a failure of all proteins to be properly localized during prophase; yet localization was normal by metaphase (Figure S2), most likely by a microtubule-dependent mechanism (Andersen et al., 2012; Siegrist and Doe, 2005). We conclude that Wor is required to establish neuroblast polarity at prophase.

Worniu Promotes Neuroblast Survival

wor mutants have fewer neuroblasts compared to the WT brains (Figure 2B), which could be caused by neuroblast apoptosis or differentiation. To determine if this reduction was due to neuroblast apoptosis, we first used a genetic sensor for caspase-mediated apoptosis, in which caspase activity induces nuclear localization of GFP by cleaving a membrane tether (Bardet et al., 2008), and found that *wor* mutant second instar brains have multiple large GFP+ cells at where central brain neuroblasts are located, indicating an elevated level of caspase-mediated cell death (Figure S3). We next used a more general cell death marker, TUNEL staining, and the Dpn antibody to unambiguously identify neuroblasts. We found 0 ± 0 ($n = 4$ brain lobes) TUNEL+ Dpn+ neuroblasts in the WT brains; in contrast, 6.1 ± 1.7 ($n = 7$; $p < 0.0001$) TUNEL+ Dpn+ neuroblasts were observed in *wor* mutants (Figure S3). RNAi depletion of the Dronc caspase gave a significant but partial rescue of the neuroblast numbers (*wor*^{1}*/Deficiency; wor-gal4 UAS-dronc RNAi*) (Figures 2B and S3); partial rescue is probably because *wor-gal4* is only expressed in a subset of neuroblasts (84.8 ± 2.2 neuroblasts per brain lobe) or the incomplete knockdown by RNAi. We conclude that the loss of neuroblasts seen in *wor* mutants is largely due to apoptosis.

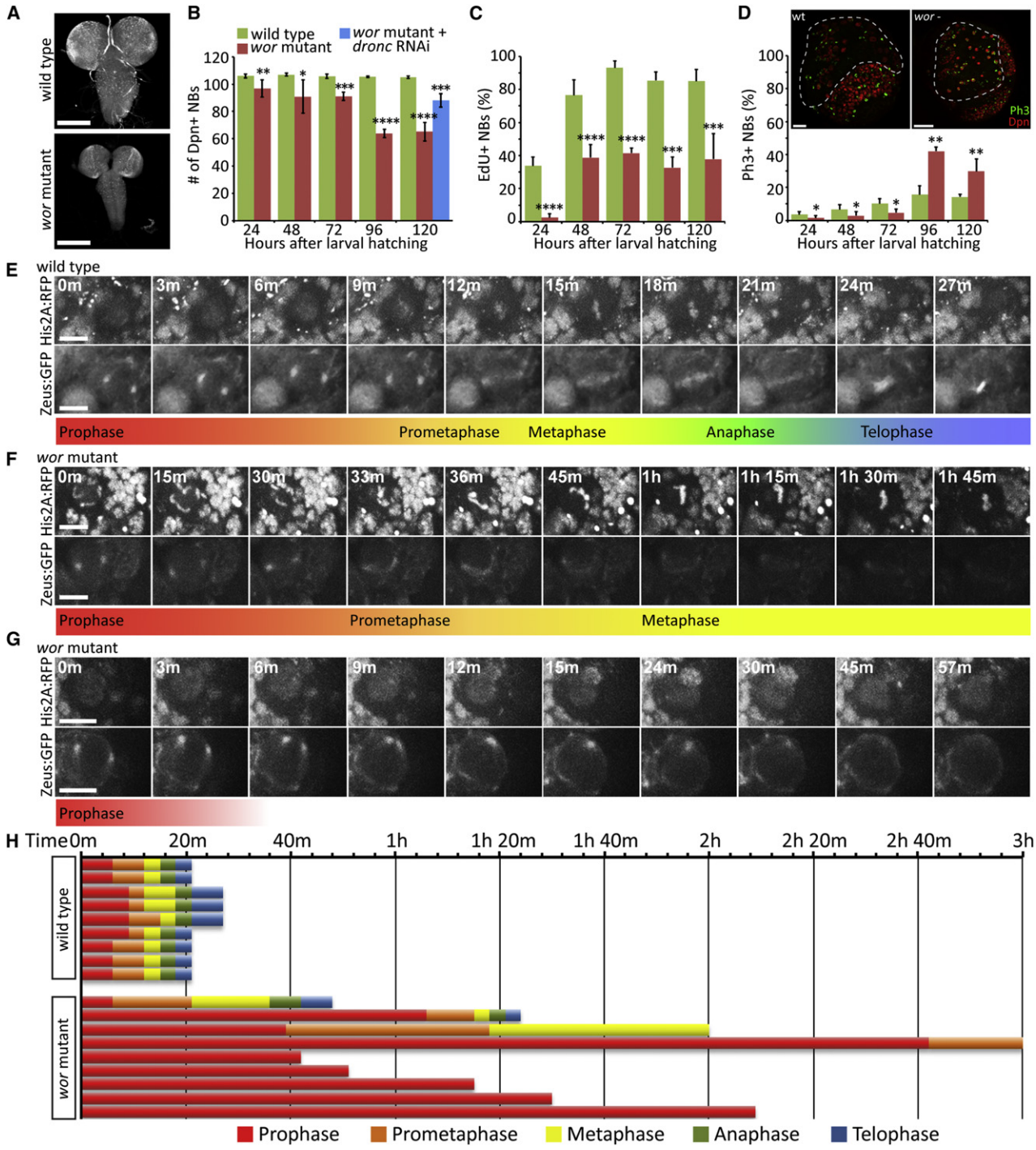

Figure 2. Worniu Is Required for Brain Development and Neuroblast Cell-Cycle Progression

(A) Merged confocal images of WT and *wor* mutant third instar larval brains stained with NB-specific marker Dpn. Scale bars represent 50 μm.

(B) Number of Dpn+ larval neuroblasts in WT (green), *wor* mutants (red), and *wor* mutant plus *dronc* RNAi (*wor*^{1}*/Deficiency; wor-gal4 UAS-dronc RNAi*) per brain lobe at the indicated developmental stages. We did not count optic lobe neuroblasts or the much smaller Dpn+ intermediate neural progenitors (Bayraktar et al., 2010; Bello et al., 2008; Boone and Doe, 2008; Bowman et al., 2008; Izergina et al., 2009). *p < 0.05; **p < 0.01; ***p < 0.001; ****p < 0.0001. P value over *wor* mutant plus *dronc* RNAi bar refers to both WT and *wor* mutant comparison.

(C) Percentage of Dpn+ larval neuroblasts that pass through S phase within the 2 hr pulse of EdU (EdU+) in WT (green) or *wor* mutants (red) at the indicated developmental stages. *p < 0.05; **p < 0.01; ***p < 0.001; ****p < 0.0001.

(D) Percentage of Dpn+ larval neuroblasts that are mitotic (PH3+) in WT (green) or *wor* mutants (red) at the indicated developmental stages. The insets show representative images of the mitotic marker phosphohistone H3 (PH3; green) and Dpn (red) staining in a WT (left panel) or a *wor* mutant brain lobe (right panel); central brain neuroblasts outlined with dashed line. *p < 0.05; **p < 0.01; ***p < 0.001; ****p < 0.0001.

worniu Mutant Neuroblasts Undergo Premature Differentiation due to an Increase in Elav Protein Levels

Based on our transcriptomic analysis, we predicted that *wor* mutant neuroblasts would show precocious neural differentiation. To determine if *wor* mutant neuroblasts initiate premature differentiation, we stained for well-characterized evolutionarily conserved neural differentiation marker Embryonic lethal abnormal visual system (Elav; Hu family in mammals); the Elav protein is normally only detected in mature postmitotic neurons where it promotes neuron-specific alternate splicing (Carney et al., 2012; Koushika et al., 1996; Lee et al., 2006; Lisbin et al., 2001; Robinow and White, 1988). Wild-type larval neuroblasts transcribe *elav* (data not shown) but have low or no Elav protein (Figure 3A; quantified in 3C), whereas many *wor* mutant neuroblasts showed detectable Elav protein (Figure 3B; quantified in 3C). We conclude that *wor* mutant neuroblasts have an abnormally high level of the Elav neuronal differentiation marker, consistent with premature differentiation.

Elav is a RNA-binding protein known to promote neuronal-specific splicing of at least three direct target genes: *neuroglian* (*nrg*), *erect wing* (*ewg*), and *armadillo* (*arm*) (Koushika et al., 2000; Lisbin et al., 2001). We counted RNA-seq reads spanning the junctions of alternatively-spliced exons of all three genes, and found that the neural-specific, Elav-dependent splice isoforms for all three transcripts were increased in *wor* mutants compared to WT (Figures 3D–3F). Thus, the increased level of Elav in *wor* mutant neuroblasts appears sufficient to bias splicing toward the neuronal-specific isoforms for all three of its known target genes.

To determine the effect of increased Elav levels on the self-renewal of *wor* mutant neuroblasts, we tested whether *wor* mutant phenotypes could be rescued by reducing Elav levels. We used *wor-gal4* to drive *UAS-elav-RNAi* in larval neuroblasts, and observed a complete rescue of the *wor* mutant cell cycle phenotype (Figures 3G and 3H) and a substantial rescue of the *wor* mutant cell polarity phenotype (Figure 3I). Thus, the increased level of Elav protein in *wor* mutant neuroblasts results in most of the cell cycle and cell polarity defects. Reducing Elav levels was not able to restore normal neuroblast numbers (Figure 3J), suggesting that it is an Elav-independent pathway. To provide an independent test for the role of Elav in neuroblast cell cycle and cell polarity, we increased Elav levels in otherwise Wt neuroblasts, and observed cell cycle and cell polarity phenotypes similar to *wor* mutants, without altering neuroblast number (Figures 3G–3J). We conclude that Wor keeps Elav protein levels low in neuroblasts, which is necessary for establishing neuroblast cell polarity and cell-cycle progression—both key stem cell features.

Worniu Overexpression Induces Nuclear Prospero and Cell-Cycle Arrest in Neuroblasts

Having established that Wor is necessary to maintain neuroblast properties (proliferation, polarity, survival), we wanted to see if ectopic Wor was sufficient to induce neuroblast attributes in GMCs or prevent neuronal differentiation. We used *prospero-gal4* to overexpress Wor in larval neuroblasts and their progeny (abbreviated as Wor^{OXN} hereafter). Unexpectedly, the Wor^{OXN} larval brains were smaller than WT brains (Figures 4A and 4B), their larval neuroblasts were smaller in diameter (Figure 4F), and the neuroblasts exhibited a severe cell cycle delay (Figure 4E). We observed no change in the number of Dpn+ central brain neuroblasts (Figure 4G). To determine the cause of the Wor^{OXN} phenotype, we tested for ectopic Prospero (Pros) protein in neuroblasts, because Pros is known to inhibit cell-cycle progression in larval neuroblasts (Bayraktar et al., 2010). Whereas both WT neuroblasts and *wor* mutant neuroblasts lack nuclear Pros (Figure 4C; data not shown), Wor^{OXN} neuroblasts had clearly detectable nuclear Pros (Figure 4D). Furthermore, when we reduced Pros levels in Wor^{OXN} larvae (Wor^{OXN}; $pros^{17}$/+) we found partial but significant rescue of the cell cycle and cell size phenotypes, and a slight increase in neuroblast numbers (Figures 4E and 4G). This latter result suggests that Wor overexpression has the ability to transform GMCs/neurons into neuroblasts, but that this is usually masked by Pros-mediated cell-cycle arrest. We conclude that overexpression of Wor does not lead to a transformation of GMC/neurons into neuroblasts, and that WT neuroblasts must precisely regulate Wor levels; too little Wor leads to Elav-induced premature differentiation, whereas too much Wor leads to Pros-induced cell-cycle arrest.

DISCUSSION

Wor and Dpn mark all neuroblasts throughout their entire lineage, yet Wor function in maintaining neuroblast biology has never been explored. Because *wor* mRNA and protein are specifically detected in neuroblasts, not in neurons or glia (Figure 1 and data not shown), the brain phenotypes described here are most likely to be due to cell autonomous function of Wor within neuroblasts. Here we show that Wor prevents premature differentiation of neuroblasts, a conclusion based in part on the upregulation of neuronal differentiation transcripts in *wor* mutant neuroblast lineages. The observed increase in neuronal differentiation transcripts is likely to be an underestimation, because *wor* mutant neuroblast lineages have three times fewer UPRT+ neurons than WT neuroblast lineages (due to the neuroblast cell-cycle delay in *wor* mutant neuroblasts; Figure 1). The reduced number of neurons in the *wor* mutant clones makes it all the more striking that we find neuronal differentiation transcripts upregulated in *wor* mutant neuroblast lineages.

A second reason we conclude that Wor prevents premature differentiation of neuroblasts is our finding that *wor* mutants have increased levels of the differentiation marker Elav within neuroblasts. How does Wor normally keep Elav protein levels low in neuroblasts? Wor may repress *elav* at the transcriptional or posttranscriptional levels. Although we see no change in

(E–G) Time-lapse imaging of larval WT (C) or *wor* mutant (D and E) neuroblasts with His2A:RFP and Zeus:GFP during mitosis. Imaging time is indicated at the upper-left corner of each frame. Cell-cycle phase is labeled below. Scale bars represent 5 μm.
(H) Cell-cycle phase lengths in WT or *wor* neuroblasts from live imaging experiments; each bar represents a single larval neuroblast. Note the lengthened prophase (red) and prometaphase (orange) in *wor* mutants.
See also Figure S3.

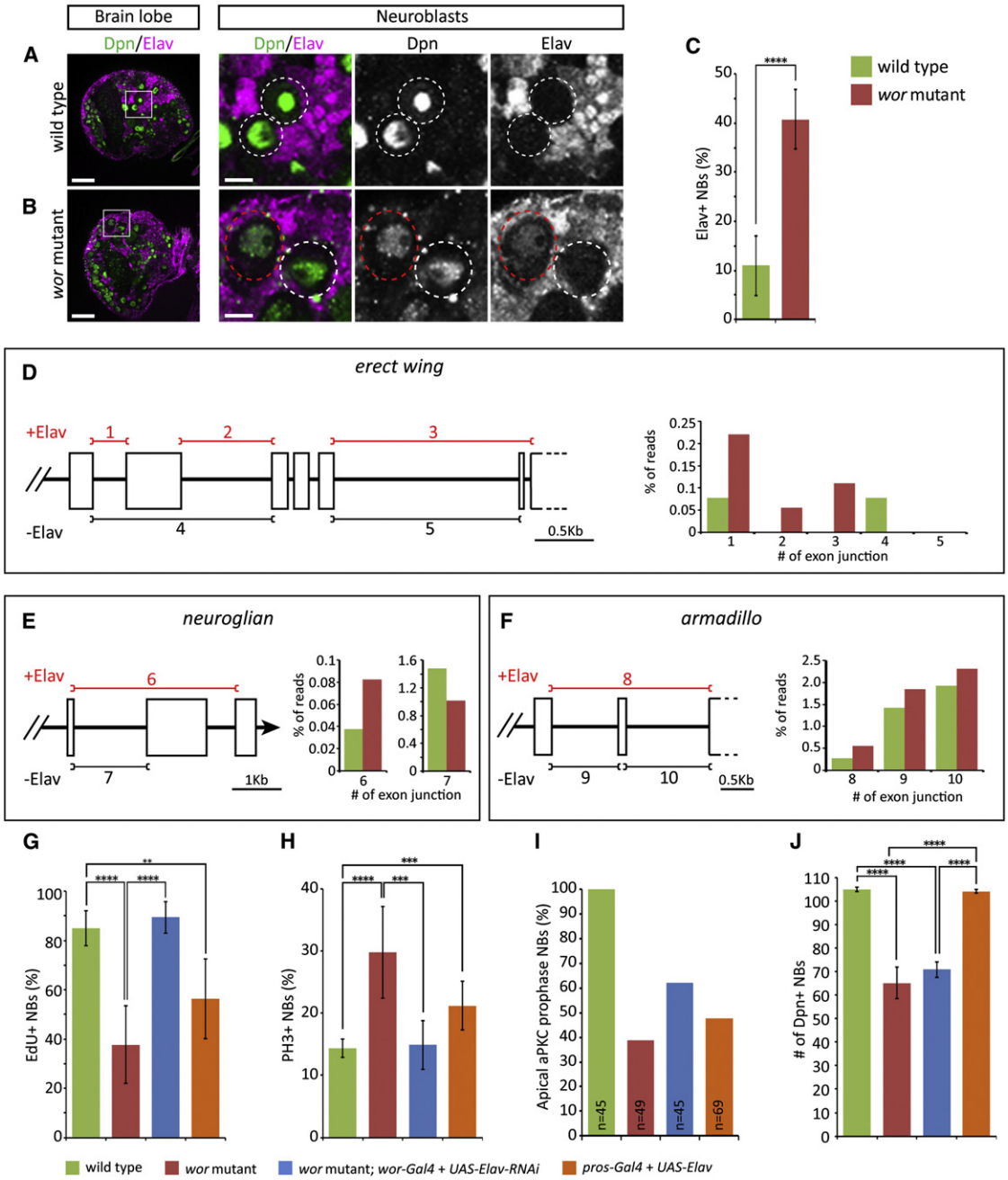

Figure 3. Worniu Represses Elav to Permit Neuroblast Cell Polarity and Cell-Cycle Progression

(A and B) Worniu represses Elav in neuroblasts. (A) Wild-type third instar larvae (96 hr ALH). (B) *wor* mutant third instar larvae (96 hr ALH). Note the detectable Elav protein in Dpn+ neuroblasts (red circle). Scale bars represent 20 μm in left panels, 5 μm in right panels.

(C) Quantification of Elav+ neuroblasts in WT and *wor* mutant larval brains. ****$p < 0.0001$.

(D–F) Elav-dependent and –independent alternative splicing junctions of *nrg*, *ewg* and *arm* and the percentage of reads spanning splicing junctions in WT and *wor* mutant RNA-seq data. Left panels show partial gene structure in the genomic region of *ewg* (X:163000-167500) for the transcripts of *ewg*-RC, *ewg*-RE, *ewg*-RF and *ewg*-RG (D), *nrg* (X:8442400..8446200) for the transcripts of *nrg*-RA and *nrg*-RB (E), and *arm* (X:1786000..1788850) for the transcripts of *arm*-RB and *arm*-RC (F). The bars represent the exon junctions used in Elav-dependent (red) or –independent manner and each junction is numbered on top or bottom of the bar. The right panels show percentage (%) of reads spanning Elav-dependent (Elav+) exon splicing junctions over total reads of each respective gene in WT (green) or in *wor* mutant (red).

(G–J) Reduction of Elav rescues *wor* mutant cell cycle and cell polarity phenotypes, whereas misexpression of Elav in WT mimics these phenotypes. (G) Neuroblasts progressing through S phase (EdU+ following a 2 hr pulse). (H) Neuroblasts in mitosis (phosphohistone H3+). (I) Neuroblasts with normal cell polarity (prophase apical aPKC crescents). (J) Number of neuroblasts. The brains were dissected from the larvae 96 hr after larval hatching. **$p < 0.01$; ***$p < 0.001$; ****$p < 0.0001$.

See also Figure S2 and Table S3.

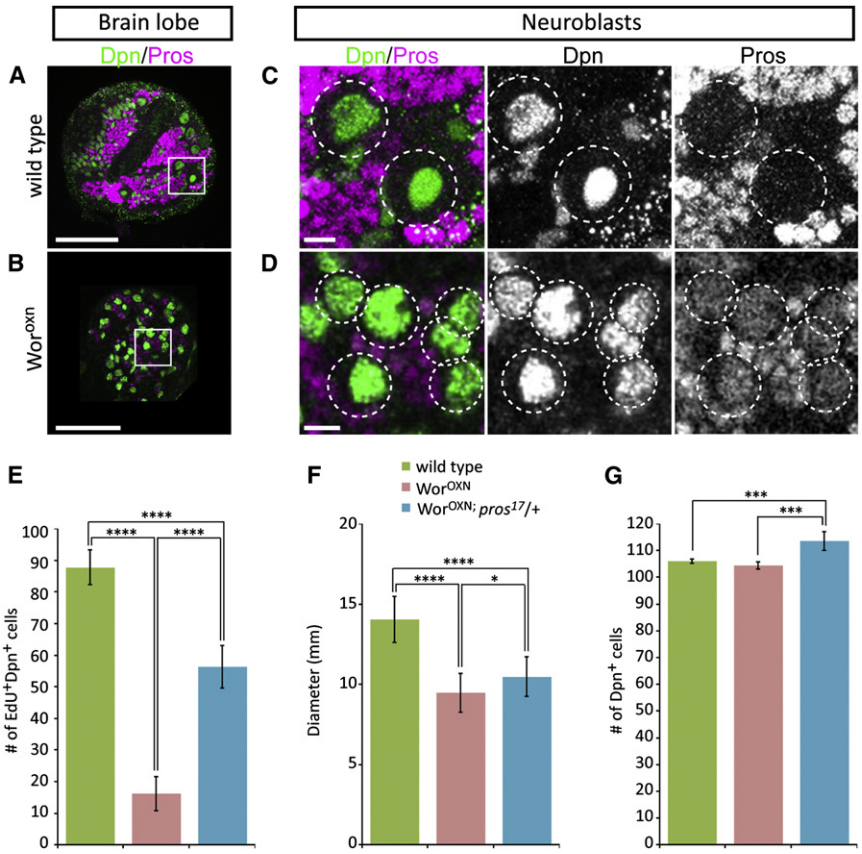

Figure 4. Worniu Misexpression in Neuroblasts Induces Nuclear Prospero and Cell-Cycle Arrest

(A–D) Worniu misexpression in neuroblasts induces nuclear Pros protein. (A,C) Wild-type third instar larvae at 96 hr ALH. (B,D) Misexpression of Wor in third instar larval Dpn+ neuroblasts (*pros-gal4 UAS-wor*; Wor^{OXN}). Both (A) and (B) are a low magnification view of a brain lobe (scale bar represents 20 μm) with the boxed region shown at high magnification of neuroblasts (dotted circles; scale bar represents 5 μm) in (C) and (D), respectively.

(E–G) Misexpression of Wor in third instar larval Dpn+ neuroblasts (*pros-gal4 UAS-wor*; Wor^{OXN}) induces cell-cycle arrest and neuroblasts size reduction without decreasing neuroblast numbers, and the phenotypes can be partially rescued by reducing Pros levels. (E) EdU incorporation following a 2hr pulse. The number of EdU+Dpn+ neuroblasts: WT, 87.8 ± 5.6; Wor^{OXN}, 16.2 ± 5.4; Wor^{OXN} *pros*^{17}/+, 56.3 ± 6.8. (F) The diameter of neuroblasts: WT, 9.5 ± 1.2 μm; Wor^{OXN}, 14.1 ± 1.4 μm; Wor^{OXN} *pros*^{17}/+, 10.8 ± 1.2 μm. (G) The neuroblast number: WT, 106.0 ± 0.8; Wor^{OXN}, 104.5 ± 1.3; Wor^{OXN} *pros*^{17}/+, 113.6 ± 3.5. *p < 0.05; ***p < 0.001; ****p < 0.0001. The brains were dissected from the larvae 96 hr after larval hatching.

elav transcript abundance between WT and *wor* mutant neuroblast lineages by RNA-seq (Table S1), *wor* mutants have three times fewer UPRT+ neurons than *wor* mutants (see above). The extra neurons in WT should result in more *elav* transcripts; the fact that we see equal levels suggests that *wor* mutant neuroblasts may have increased levels of *elav* transcription. On the other hand, Wor may repress Elav at a posttranscriptional level. Wild-type embryonic and larval neuroblasts transcribe the *elav* gene but little of the mRNA is translated (Berger et al., 2007) (data not shown); it is likely that *elav* is also posttranscriptionally regulated in larval neuroblasts, and this step could be subject to direct or indirect regulation by Wor. Thus, Wor may regulate *elav* at the transcriptional and/or posttranscriptional level to keep Elav protein low in neuroblasts.

How does Elav promote premature differentiation of neuroblasts? Elav may act by inducing neuronal-specific splicing of its direct targets *neuroglian, erect wing*, and *armadillo* (which we observe to be upregulated in *wor* mutants), or additional targets that have yet to be identified. In addition, other RNA splicing factors, many of which are up- or downregulated at least 2-fold in *wor* mutants (Table S1), may coregulate Elav targets and/or splicing of additional pre-mRNAs. Genomic analysis of alternative splicing junction usage in *wor* mutants showed a profound change of global splicing events: 15.0% of all potentially alternatively-spliced exons (14,476 junctions from 3,430 genes; see Experimental Procedures) showed >2-fold change in *wor* mutants compared to WT (Table S3). Because the function of different splice isoforms are so poorly understood, we can only speculate that some or all of the upregulated splice isoforms promote neural differentiation and inhibit cell cycle in *wor* mutants. Neuronal differentiation seen in *wor* mutant neuroblasts is not complete, because *wor* mutant neuroblasts maintain expression of neuroblast markers such as Dpn, Ase, and Miranda (data not shown). Thus, *wor* mutant neuroblasts have a mixed fate, in which both neuroblast and neuronal genes are expressed.

Wor is required to promote cell polarity at prophase. The defect in apical protein localization seen in *wor* mutants is similar to that seen in the absence of an external polarizing cue in embryonic neuroblasts (Siegrist and Doe, 2006, 2007; Yoshiura et al., 2012), or in *sgt1* mutant larval neuroblasts (Andersen et al., 2012). It is also coincident with the prophase cell-cycle delay observed by live imaging, but the relationship between loss of polarity proteins and prophase delay is unknown. Wor is also required to prevent neuroblast apoptosis. In mammals, Snail family members are known to protect cells from apoptosis triggered by loss of survival signals (Vega et al., 2004). It remains unknown whether Wor acts in a similar manner; all we can say is that Wor acts via an Elav-independent pathway to maintain neuroblast survival.

Wor is required for cell-cycle progression from prophase to metaphase. It is interesting that loss of *wor* causes cell-cycle delays at the precise time when the microtubule cytoskeleton is dramatically reorganized into a bipolar spindle. In addition, our RNA-seq data shows that *wor* mutants are depleted for "microtubule cytoskeleton organization" annotated transcripts (Figure 1I). Mammalian Snail family proteins confer migratory properties to epithelial cells during EMT or metastasis, which also involves a dramatic reorganization of the cytoskeleton

(Barrallo-Gimeno and Nieto, 2005; Cano et al., 2000; Nieto, 2011). Thus, Wor may have a conserved function in regulating the microtubule cytoskeleton. Because reducing Elav levels can rescue cell-cycle progression, Wor appears to regulate the microtubule cytoskeleton indirectly, via keeping Elav protein levels low. High levels of Elav in neuroblasts may induce microtubule organization characteristic of mature neurons, such as using a single centrosome to nucleate unidirectional microtubule outgrowth into the axon. Thus, neuroblasts with high levels of Elav may be unable to efficiently duplicate their centrosomes or form a bipolar mitotic spindle, leading to the observed prophase arrest phenotype.

EXPERIMENTAL PROCEDURES

Fly Genetics

See Supplemental Experimental Procedures.

TU-Tagging, RNA-seq, and RNA Sequence Analysis

TU-tagging is a method for labeling of newly transcribed RNAs in cells containing the *Toxoplasma gondii* enzyme UPRT and exposed to 4-thiouracil (4TU) (Miller et al., 2009; Zeiner et al., 2008). Larvae were raised at 25°C. After 3 days, 50 larvae were transferred to agar plates with 500 μM 4-thiouracil (Sigma, St. Louis, MO) for 5 hr. We added 1 mM oxonic acid (Sigma) to avoid a salvage pathway which can use 4-thiouracil without the presence of UPRT (M. Cleary, personal communication). Standard methods were used to purify RNA (Miller et al., 2009; Zeiner et al., 2008). For each experiment, 5–10 ng of streptavidin purified (TU-tagged) RNA was converted to double stranded cDNA (ds-cDNA) using the Ovation RNA-seq System V2 (NuGEN), and 1 μg of ds-cDNA was used to generate an indexed Illumina library using NEBNext DNA Sample Prep Master Mix Set 1 (NE BioLabs). The resulting libraries were sequenced together in one lane of an HiSeq 2000 using version 3 sequencing reagents. This resulted in 13.7–14.8 million single-end 100 bp reads from each indexed library. The sequence reads were aligned against the *D melanogaster* release 5 genome sequence using Bowtie 2 (http://bowtie-bio.sourceforge.net/bowtie2/) in "sensitive-local" mode, and the number of reads mapping to each gene region or each alternatively spliced exon junction of the release 5.25 genome annotation was determined using the SAMtools (Li et al., 2009) "view" command. Reads per million (RPM) expression values were calculated by normalizing the number of reads that mapped to each gene region or each alternatively spliced exon junction to the total number of reads that mapped to all gene regions. RPM values from biological replicate experiments were averaged.

Dissection, Antibody and TUNEL Staining, EdU Incorporation, and Time-Lapse Imaging

Antibody staining followed published protocols (Lee et al., 2006). Primary antibodies: rat anti-Pins; rat anti-Dpn; guinea pig anti-bazooka; guinea pig anti-Mira; rat anti-Mira; mouse anti-Pros; rabbit anti-PH3; rabbit anti-aPKC; mouse anti-α-tubulin; guinea pig anti-Numb; mouse anti-Insc; mouse anti-Elav (details in Supplemental Experimental Procedures). TUNEL staining was done by manufacture's protocol (Roche, Indianapolis, IN). For EdU incorporation, larval brains explants were incubated in S2 medium (Sigma) containing 100 μg/mL EdU (Molecular Probes, Eugene, OR) at 25°C for 2 hr. After completing standard fixation and antibody staining procedures, EdU was detected by following manufacturer's protocols (Molecular Probes). Microscopy was done using a Zeiss LSM700, and images were processed with FIJI (http://fiji.sc). Time-lapse imaging was done by standard protocols using a Leica spinning disc microscope (Siller et al., 2005) and montaged with FIJI. All quantifications are presented as average ± SD.

SUPPLEMENTAL INFORMATION

Supplemental Information includes three figures, three tables, and Supplemental Experimental Procedures and can be found with this article online at http://dx.doi.org/10.1016/j.devcel.2012.09.007.

ACKNOWLEDGMENTS

We thank L. Gay, C. Cabernard, R. Andersen, and J. Kroll for technical assistance; Tory Herman, Yan Yan, Omer Bayraktar, Travis Carney, Minoree Kohwi, Tony Ip, and Alex Gould for comments on the manuscript; and Jim Skeath and Bill Chia for antibodies. The work was supported by HHMI, where C.Q.D. is an investigator.

Received: May 4, 2012
Revised: July 17, 2012
Accepted: September 12, 2012
Published online: October 15, 2012

REFERENCES

Andersen, R.O., Turnbull, D.W., Johnson, E.A., and Doe, C.Q. (2012). Sgt1 acts via an LKB1/AMPK pathway to establish cortical polarity in larval neuroblasts. Dev. Biol. *363*, 258–265.

Ashraf, S.I., and Ip, Y.T. (2001). The Snail protein family regulates neuroblast expression of inscuteable and string, genes involved in asymmetry and cell division in Drosophila. Development *128*, 4757–4767.

Ashraf, S.I., Hu, X., Roote, J., and Ip, Y.T. (1999). The mesoderm determinant snail collaborates with related zinc-finger proteins to control Drosophila neurogenesis. EMBO J. *18*, 6426–6438.

Ashraf, S.I., Ganguly, A., Roote, J., and Ip, Y.T. (2004). Worniu, a Snail family zinc-finger protein, is required for brain development in Drosophila. Dev. Dyn. *231*, 379–386.

Bardet, P.L., Kolahgar, G., Mynett, A., Miguel-Aliaga, I., Briscoe, J., Meier, P., and Vincent, J.P. (2008). A fluorescent reporter of caspase activity for live imaging. Proc. Natl. Acad. Sci. USA *105*, 13901–13905.

Barrallo-Gimeno, A., and Nieto, M.A. (2005). The Snail genes as inducers of cell movement and survival: implications in development and cancer. Development *132*, 3151–3161.

Bayraktar, O.A., Boone, J.Q., Drummond, M.L., and Doe, C.Q. (2010). Drosophila type II neuroblast lineages keep Prospero levels low to generate large clones that contribute to the adult brain central complex. Neural Dev. *5*, 26.

Bello, B.C., Izergina, N., Caussinus, E., and Reichert, H. (2008). Amplification of neural stem cell proliferation by intermediate progenitor cells in Drosophila brain development. Neural Dev. *3*, 5.

Berger, C., Renner, S., Lüer, K., and Technau, G.M. (2007). The commonly used marker ELAV is transiently expressed in neuroblasts and glial cells in the Drosophila embryonic CNS. Dev. Dyn. *236*, 3562–3568.

Boone, J.Q., and Doe, C.Q. (2008). Identification of Drosophila type II neuroblast lineages containing transit amplifying ganglion mother cells. Dev. Neurobiol. *68*, 1185–1195.

Bowman, S.K., Rolland, V., Betschinger, J., Kinsey, K.A., Emery, G., and Knoblich, J.A. (2008). The tumor suppressors Brat and Numb regulate transit-amplifying neuroblast lineages in Drosophila. Dev. Cell *14*, 535–546.

Cabernard, C., and Doe, C.Q. (2009). Apical/basal spindle orientation is required for neuroblast homeostasis and neuronal differentiation in Drosophila. Dev. Cell *17*, 134–141.

Cabernard, C., Prehoda, K.E., and Doe, C.Q. (2010). A spindle-independent cleavage furrow positioning pathway. Nature *467*, 91–94.

Cai, Y., Chia, W., and Yang, X. (2001). A family of snail-related zinc finger proteins regulates two distinct and parallel mechanisms that mediate Drosophila neuroblast asymmetric divisions. EMBO J. *20*, 1704–1714.

Cano, A., Pérez-Moreno, M.A., Rodrigo, I., Locascio, A., Blanco, M.J., del Barrio, M.G., Portillo, F., and Nieto, M.A. (2000). The transcription factor snail controls epithelial-mesenchymal transitions by repressing E-cadherin expression. Nat. Cell Biol. *2*, 76–83.

Carney, T.D., Miller, M.R., Robinson, K.J., Bayraktar, O.A., Osterhout, J.A., and Doe, C.Q. (2012). Functional genomics identifies neural stem cell subtype expression profiles and genes regulating neuroblast homeostasis. Dev. Biol. *361*, 137–146.

Chabu, C., and Doe, C.Q. (2008). Dap160/intersectin binds and activates aPKC to regulate cell polarity and cell cycle progression. Development *135*, 2739–2746.

Doe, C.Q. (2008). Neural stem cells: balancing self-renewal with differentiation. Development *135*, 1575–1587.

Izergina, N., Balmer, J., Bello, B., and Reichert, H. (2009). Postembryonic development of transit amplifying neuroblast lineages in the Drosophila brain. Neural Dev. *4*, 44.

Knoblich, J.A. (2008). Mechanisms of asymmetric stem cell division. Cell *132*, 583–597.

Koushika, S.P., Lisbin, M.J., and White, K. (1996). ELAV, a Drosophila neuron-specific protein, mediates the generation of an alternatively spliced neural protein isoform. Curr. Biol. *6*, 1634–1641.

Koushika, S.P., Soller, M., and White, K. (2000). The neuron-enriched splicing pattern of Drosophila erect wing is dependent on the presence of ELAV protein. Mol. Cell. Biol. *20*, 1836–1845.

Lee, C.Y., Robinson, K.J., and Doe, C.Q. (2006). Lgl, Pins and aPKC regulate neuroblast self-renewal versus differentiation. Nature *439*, 594–598.

Li, H., Handsaker, B., Wysoker, A., Fennell, T., Ruan, J., Homer, N., Marth, G., Abecasis, G., and Durbin, R.; 1000 Genome Project Data Processing Subgroup. (2009). The Sequence Alignment/Map format and SAMtools. Bioinformatics *25*, 2078–2079.

Lisbin, M.J., Qiu, J., and White, K. (2001). The neuron-specific RNA-binding protein ELAV regulates neuroglian alternative splicing in neurons and binds directly to its pre-mRNA. Genes Dev. *15*, 2546–2561.

Miller, M.R., Robinson, K.J., Cleary, M.D., and Doe, C.Q. (2009). TU-tagging: cell type-specific RNA isolation from intact complex tissues. Nat. Methods *6*, 439–441.

Nieto, M.A. (2002). The snail superfamily of zinc-finger transcription factors. Nat. Rev. Mol. Cell Biol. *3*, 155–166.

Nieto, M.A. (2011). The ins and outs of the epithelial to mesenchymal transition in health and disease. Annu. Rev. Cell Dev. Biol. *27*, 347–376.

Roark, M., Sturtevant, M.A., Emery, J., Vaessin, H., Grell, E., and Bier, E. (1995). scratch, a pan-neural gene encoding a zinc finger protein related to snail, promotes neuronal development. Genes Dev. *9*, 2384–2398.

Robinow, S., and White, K. (1988). The locus elav of Drosophila melanogaster is expressed in neurons at all developmental stages. Dev. Biol. *126*, 294–303.

Schuh, M., Lehner, C.F., and Heidmann, S. (2007). Incorporation of Drosophila CID/CENP-A and CENP-C into centromeres during early embryonic anaphase. Curr. Biol. *17*, 237–243.

Siegrist, S.E., and Doe, C.Q. (2005). Microtubule-induced Pins/Galphai cortical polarity in Drosophila neuroblasts. Cell *123*, 1323–1335.

Siegrist, S.E., and Doe, C.Q. (2006). Extrinsic cues orient the cell division axis in Drosophila embryonic neuroblasts. Development *133*, 529–536.

Siegrist, S.E., and Doe, C.Q. (2007). Microtubule-induced cortical cell polarity. Genes Dev. *21*, 483–496.

Siller, K.H., and Doe, C.Q. (2008). Lis1/dynactin regulates metaphase spindle orientation in Drosophila neuroblasts. Dev. Biol. *319*, 1–9.

Siller, K.H., Serr, M., Steward, R., Hays, T.S., and Doe, C.Q. (2005). Live imaging of Drosophila brain neuroblasts reveals a role for Lis1/dynactin in spindle assembly and mitotic checkpoint control. Mol. Biol. Cell *16*, 5127–5140.

Siller, K.H., Cabernard, C., and Doe, C.Q. (2006). The NuMA-related Mud protein binds Pins and regulates spindle orientation in Drosophila neuroblasts. Nat. Cell Biol. *8*, 594–600.

Thiery, J.P., Acloque, H., Huang, R.Y., and Nieto, M.A. (2009). Epithelial-mesenchymal transitions in development and disease. Cell *139*, 871–890.

Vega, S., Morales, A.V., Ocaña, O.H., Valdés, F., Fabregat, I., and Nieto, M.A. (2004). Snail blocks the cell cycle and confers resistance to cell death. Genes Dev. *18*, 1131–1143.

Yoshiura, S., Ohta, N., and Matsuzaki, F. (2012). Tre1 GPCR signaling orients stem cell divisions in the Drosophila central nervous system. Dev. Cell *22*, 79–91.

Zeiner, G.M., Cleary, M.D., Fouts, A.E., Meiring, C.D., Mocarski, E.S., and Boothroyd, J.C. (2008). RNA analysis by biosynthetic tagging using 4-thiouracil and uracil phosphoribosyltransferase. Methods Mol. Biol. *419*, 135–146.